The Upper Mantle and Transition Zone:

Computation of Phase Relations and Elastic Properties

Craig R. Bina* and B. J. Wood

Department of Geological Sciences, Northwestern University, Evanston, Illinois

To Be Submitted to: *Reviews of Geophysics*

DRAFT: 17 July 1987

*Now at: Geophysical Institute, Faculty of Science, University of Tokyo, Bunkyo, Tokyo 113, Japan.

The Upper Mantle and Transition Zone:

Computation of Phase Relations and Elastic Properties

Craig R. Bina* and B. J. Wood

Department of Geological Sciences, Northwestern University, Evanston, Illinois

Abstract. We review the details of the thermodynamic formalism required for the determination of internally consistent phase diagrams and for the calculation of stable phase assemblages and their associated elastic properties. We apply the method to the computation of seismic velocity profiles for a suite of upper mantle models ranging in bulk composition from eclogitic through peridotitic to pure olivine, incorporating recent data on the pyroxene-garnet system. We conclude that there is no need to invoke arbitrary changes in the bulk chemical composition of the upper mantle; a uniform peridotitic upper mantle containing 70-75% olivine by volume is in good agreement with upper mantle seismic observations. The details of various numerical procedures necessary to the performance of such thermodynamic analyses are presented in Appendices.

Introduction

Radial variations in the velocities of seismic wave propagation in the upper mantle of the Earth are diagnostic of changes in the elastic properties of the materials comprising the planet's interior. These variations may be ascribed to changes in the bulk chemical composition of the interior [*e.g.*, Bullen, 1937], or they may be due to the occurrence of structural transformations in material of uniform bulk chemical composition [*e.g.*, Bernal, 1936]. The principle of Occam's Razor [*cf.* Hamilton, 1837; Albutt, 1901] dictates that we should not invoke additional free parameters (*i.e.*, arbitrary changes in bulk composition) unless the simpler hypothesis (*i.e.*, a uniform composition) is insufficient to explain the observations. Thus, here we examine the two primary families of phase transitions (eclogite-garnetite and olivine-spinel) which are observed to occur in the laboratory under upper mantle conditions [*cf.* Ringwood, 1975] in order to determine whether their respective characteristics are sufficient to explain upper mantle seismic observations.

*Now at: Geophysical Institute, Faculty of Science, University of Tokyo, Bunkyo, Tokyo 113, Japan.

Experimental data on the thermodynamic properties of minerals can be used to predict stable phase assemblages and mineral compositions as general functions of pressure, temperature, and bulk chemical composition. Given suitable thermoelastic data, additional physical properties — such as density or seismic velocities — can also be predicted for the various stable phase assemblages. These predicted properties can then be compared with actual observations — of phase distribution, mineral composition, density, or seismic velocities — made on natural systems in order to determine whether the model pressure, temperature, or bulk chemical composition is appropriate to the system under investigation [*cf.* Bina and Wood, 1984, 1986, 1987]. By thus combining independent data from calorimetric studies, phase equilibrium experiments, low temperature elastic constant measurements, and seismic observations and applying these data together in an internally consistent fashion, we can place tighter constraints upon mantle compositions than if we were to apply them in isolation.

Here we first review the techniques of calculating chemical potentials of mineral phases as explicit functions of pressure, temperature, and composition. We then discuss the use of these chemical potential formulations in computing internally consistent phase diagrams for simple systems and in determining stable phase assemblages, mineral compositions, and aggregate elastic properties for complex multi-component systems. Finally, we present as an example the computation of equilibrium mineralogies and associated seismic velocity structures for a suite of upper mantle model bulk compositions, ranging from eclogite to pure olivine, and their comparison with observed transition zone seismic velocity profiles. In Appendix A we discuss the calculation of divariant and univariant phase relations; in Appendix B we discuss the computation of stable phase assemblages by the method of free energy minimization, and in Appendix C we briefly review the use of Newton's method for the solution of non-linear equations.

Computing Chemical Potentials

In order to perform thermodynamic calculations with intent to determine phase equilibrium properties, we must have some quantitative measure of the relative stabilities of mineral phases. For this purpose we make use of the ''chemical potential'', $\bar{G}_i^{\phi}$, of a component i in the phase ϕ. This chemical potential is defined [Denbigh, 1981, p. 79] as the partial molar Gibbs free energy,

$$\bar{G}_i^{\phi} \equiv \left(\frac{\partial G^{\phi}}{\partial n_i^{\phi}} \right)_{P,T} ,$$

where G^{ϕ} is the Gibbs free energy of phase ϕ; n_i^{ϕ} is the number of moles of component i in phase ϕ, and P and T are the pressure and temperature of interest, respectively. The chemical potential [*cf.* Denbigh, 1981, pp. 98-104] may be expressed as a function of pressure, temperature, and composition:

$$\bar{G}_i^{\phi} = {}^{i\phi}\bar{H}_T^{o} - T\,{}^{i\phi}\bar{S}_T^{o} + \int_1^P {}^{i\phi}\bar{V}_T^{o}(\hat{P})d\hat{P} + RT \ln {}^{i\phi}a_{P,T}(X_i^{\phi}) . \quad (1)$$

Here, ${}^{i\phi}\bar{H}_T^{o}$ and ${}^{i\phi}\bar{S}_T^{o}$ are the partial molar enthalpy and entropy, respectively, of pure (''standard state'') component i in phase ϕ at temperature T; ${}^{i\phi}\bar{V}_T^{o}(\hat{P})$ is the partial molar volume of pure component i in phase ϕ at temperature T and pressure $\hat{P}$; ${}^{i\phi}a_{P,T}(X_i^{\phi})$ is the activity of component i in phase ϕ at temperature T, pressure P, and composition X_i^{ϕ}; X_i^{ϕ} is the mole fraction of component i in phase ϕ, and R is the universal gas constant.

Enthalpy and Entropy Terms

Data on the enthalpy and entropy of a component are available at 1 bar and some reference temperature, T_0. We correct these values to the temperature of interest, T, as follows:

$${}^{i\phi}\bar{H}_T^{o} = {}^{i\phi}\bar{H}_{T_0}^{o} + \int_{T_0}^{T} {}^{i\phi}\overline{C_P}(\hat{T})d\hat{T}$$

$${}^{i\phi}\bar{S}_T^{o} = {}^{i\phi}\bar{S}_{T_0}^{o} + \int_{T_0}^{T} \frac{1}{\hat{T}}\,{}^{i\phi}\overline{C_P}(\hat{T})d\hat{T} ,$$

where ${}^{i\phi}\overline{C_P}(\hat{T})$ is the partial molar isobaric heat capacity of pure component i in phase ϕ and is itself generally a function of temperature. (For solid-solid phase relations, an extremely good simplification is that the heat capacity difference between high and low pressure phases is independent of temperature [Wood and Holloway, 1984]. This is equivalent to fixing all of the heat capacities at their values for the reference temperature, T_0.)

Volume Term

The molar volume of a component is generally available at 1 bar and some reference temperature, T_0. We first correct for the temperature of interest, T:

$$ {}^{i\phi}\bar{V}^{o}_{T}(1\ \text{bar}) = {}^{i\phi}\bar{V}^{o}_{T_0}(1\ \text{bar}) \cdot \exp\left[\int_{T_0}^{T} {}^{i\phi}\alpha(\hat{T})d\hat{T}\right], $$

where ${}^{i\phi}\alpha(\hat{T})$ is the volume coefficient of thermal expansion of pure component i in phase ϕ and is itself generally a function of temperature. (At moderate temperatures ${}^{i\phi}\alpha$ is expected to increase linearly with T, attaining a limiting value at high temperatures [*cf.* Ashcroft and Mermin, 1976, pp. 490-495].) We next correct for the pressure of interest, P, making use of the third-order Birch-Murnaghan equation based upon the finite strain formulation of Birch [1952]:

$$ P = 3\ {}^{i\phi}K_T^{(1,T)} f \left[1 + 2f\right]^{\frac{5}{2}} \left[1 - 2\xi f\right], \qquad (2) $$

where:

$$ f \equiv \frac{1}{2}\left[\left(\frac{{}^{i\phi}\bar{V}^{o}_{T}(1)}{{}^{i\phi}\bar{V}^{o}_{T}(P)}\right)^{\frac{2}{3}} - 1\right] $$

$$ \xi \equiv \frac{3}{4}\left[4 - \left\{\frac{d^{i\phi}K_T}{dP}\right\}\right]. $$

Here ${}^{i\phi}K_T^{(1,T)}$ is the isothermal bulk modulus (''incompressibility'') of pure component i in phase ϕ at 1 bar and temperature T. This value, and its pressure derivative, are obtained from the generally available adiabatic bulk modulus (and its pressure derivative) at 1 bar and a reference temperature T_0, ${}^{i\phi}K_T^{(1,T_0)}$, via the relationships:

$$ {}^{i\phi}K_T^{(1,T)} = {}^{i\phi}K_S^{(1,T)} \cdot \left[1 + T\ {}^{i\phi}\alpha(T)\ {}^{i\phi}\gamma\right]^{-1} $$

$$ \left\{\frac{d^{i\phi}K_T}{dP}\right\} = \left\{\frac{d^{i\phi}K_S}{dP}\right\} \cdot \left[1 + T\ {}^{i\phi}\alpha(T)\ {}^{i\phi}\gamma\right]^{-1} \boxed{- K_T T \cdot d[{}^{i\varphi}\alpha(T){}^{i\varphi}\gamma]/dP \cdot [1+T{}^{i\varphi}\alpha(T){}^{i\varphi}\gamma]^{-1}} $$

where:

$$ {}^{i\phi}K_S^{(1,T)} = {}^{i\phi}K_S^{(1,T_0)} \cdot \exp\left[-\ {}^{i\phi}\delta_S \int_{T_0}^{T} {}^{i\phi}\alpha(\hat{T})d\hat{T}\right]. \qquad (3) $$

In the equations above, the Grüneisen ratio ${}^{i\phi}\gamma$ and the Anderson-Grüneisen parameter ${}^{i\phi}\delta_S$ for pure component i in phase ϕ are given by:

$$ {}^{i\phi}\delta_S = \frac{-1}{{}^{i\phi}\alpha\ {}^{i\phi}K_S}\left(\frac{\partial {}^{i\phi}K_S}{\partial T}\right)_P $$

$$ {}^{i\phi}\gamma = \frac{{}^{i\phi}\alpha\ {}^{i\phi}K_S\ {}^{i\phi}\bar{V}^{o}}{{}^{i\phi}C_P}. $$

Given, then, this formulation for the pressure dependence of the molar volume, we must now integrate equation

(2) in pressure in order to obtain the $\int VdP$ term in equation (1). Since equation (2) is an implicit function for V(P), we choose [G. Helffrich, pers. comm., 1987] to integrate it by parts:

$$\int_1^P {}^{i\phi}\bar{V}_T^o(\hat{P})d\hat{P} = \hat{P}\ {}^{i\phi}\bar{V}_T^o(\hat{P})\Big|_{\hat{P}=1}^{P} - \int_{{}^{i\phi}\bar{V}_T^o(1)}^{{}^{i\phi}\bar{V}_T^o(P)} P(\hat{V})d\hat{V}$$

$$= \frac{3}{2}\ {}^{i\phi}K_T^{(1,T)} \left\{ \left[\frac{9}{8}\left[\frac{d^{i\phi}K_T}{dP}\right] - \frac{9}{2} \right] \left[{}^{i\phi}\bar{V}_T^o(1)\right]^3 \left[{}^{i\phi}\bar{V}_T^o(P)\right]^{-2} \right.$$

$$+ \left[\frac{49}{4} - \frac{21}{8}\left[\frac{d^{i\phi}K_T}{dP}\right] \right] \left[{}^{i\phi}\bar{V}_T^o(1)\right]^{\frac{7}{3}} \left[{}^{i\phi}\bar{V}_T^o(P)\right]^{\frac{-4}{3}}$$

$$\left. + \left[\frac{15}{8}\left[\frac{d^{i\phi}K_T}{dP}\right] - 10 \right] \left[{}^{i\phi}\bar{V}_T^o(1)\right]^{\frac{5}{3}} \left[{}^{i\phi}\bar{V}_T^o(P)\right]^{\frac{-2}{3}} - \left[\frac{3}{8}\left[\frac{d^{i\phi}K_T}{dP}\right] - \frac{9}{4} \right] {}^{i\phi}\bar{V}_T^o(1) \right\},$$

where we obtain ${}^{i\phi}\bar{V}_T^o(P)$ by solution of equation (2) using a one-dimensional Newton's method (see Appendix C).

Activity Term

Finally, we require a relationship between the activity ${}^{i\phi}a_{P,T}$ of component i in phase ϕ and the composition X_i^ϕ of phase ϕ, where X_i^ϕ is the mole fraction of component i in phase ϕ. These activity-composition relationships are of the form:

$${}^{i\phi}a_{P,T} = f_\phi\left[X_i^\phi, P, T\right],$$

where f_ϕ is a function whose form depends upon the details of crystal structure and inter-site interactions. Activity-composition functions for pyroxene components are presented by Wood and Holloway [1982, 1984], and those for garnets are discussed by Haselton and Newton [1980], Wood and Holloway [1982, 1984], and Bina and Wood [1984]. Such relationships for olivine components are presented by Fisher and Medaris [1969] and Wood and Kleppa [1981] while functions for the β and γ polymorphs are given by Bina and Wood [1987].

Computing Phase Equilibria in Simple Systems

Given formulations for the chemical potentials of components as functions of pressure, temperature, and composition (equation (2)), we may now proceed to the calculation of phase equilibria in simple systems. Con-

sider a system of two components, 1 and 2, and two mineral phases, α and γ; we wish to determine the conditions of pressure, temperature, and mineral composition under which the two phase α and γ can coexist at equilibrium. At equilibrium, the chemical potential of a given component must be the same in all phases [*cf.* Denbigh, 1981, p.86], thus:

$$\begin{cases} \bar{G}_1^{\alpha}(P,T,X_1^{\alpha}) = \bar{G}_1^{\gamma}(P,T,X_1^{\gamma}) \\ \bar{G}_2^{\alpha}(P,T,X_2^{\alpha}) = \bar{G}_2^{\gamma}(P,T,X_2^{\gamma}) \ . \end{cases} \tag{4}$$

Since $X_2^{\alpha} = 1 - X_1^{\alpha}$ and $X_2^{\gamma} = 1 - X_1^{\gamma}$, we effectively have two equations in four unknowns: P, T, X_1^{α}, and X_1^{γ}. At any given pressure and temperature then, equations (4) reduce to two equations in two unknowns, and we may solve them by a two-dimensional Newton's method (see Appendix A) for the compositions X_1^{α} and X_1^{γ} at which the phases α and γ can coexist in equilibrium. In Figure 2-3, for example, we have computed, at 1000°C, the compositions at which α-olivine and γ-spinel may coexist over a broad range of pressures, thus defining the ''α+γ'' divariant loop shown in that figure.

This procedure may be extended to the computation of the conditions under which three phases, α, β, and γ, may coexist in a binary system. In this case, equations (4) become:

$$\begin{cases} \bar{G}_1^{\alpha}(P,T,X_1^{\alpha}) = \bar{G}_1^{\beta}(P,T,X_1^{\beta}) \\ \bar{G}_1^{\alpha}(P,T,X_1^{\alpha}) = \bar{G}_1^{\gamma}(P,T,X_1^{\gamma}) \\ \bar{G}_2^{\alpha}(P,T,X_2^{\alpha}) = \bar{G}_2^{\beta}(P,T,X_2^{\beta}) \\ \bar{G}_2^{\alpha}(P,T,X_2^{\alpha}) = \bar{G}_2^{\gamma}(P,T,X_2^{\gamma}) \ . \end{cases} \tag{5}$$

Again, $X_2^{\alpha} = 1 - X_1^{\alpha}$, $X_2^{\beta} = 1 - X_1^{\beta}$, and $X_2^{\gamma} = 1 - X_1^{\gamma}$, so we have four equations in five unknowns: P, T, X_1^{α}, X_1^{β}, and X_1^{γ}. At any given temperature then, equations (5) reduce to four equations in four unknowns, and we may solve for the compositions X_1^{α}, X_1^{β}, and X_1^{γ} and the pressure P at which the three phases can coexist in equilibrium by using a four-dimensional Newton's method (see Appendix A). This is illustrated as well in Figure 2-3, where we have computed the compositions and pressure at which α-olivine, β-modified-spinel, and γ-spinel can all coexist in stable equilibrium at 1000°C, thus defining the α+β+γ univariant line shown in that figure.

Hence, by this procedure we may compute a phase diagram, such as Figure 2-3, for a simple system from a set of thermodynamic data. Independent of these data, there may be available data from ''phase equilibrium experiments''. Such data, shown by the polygonal symbols in Figure 2-3, directly indicate which phases can

coexist in equilibrium at specific conditions of pressure, temperature, and composition. Thus, if such experimental data have truly demonstrated equilibrium (*e.g.*, by ''reversibility'' [Fyfe, 1960]), they serve as independent delimiters of the stability fields in the phase diagram. For a phase diagram to be internally consistent, these two independent constraints upon the topology of the phase diagram must agree. For example, any experimental points at which only γ phase is stable must lie in the computed γ phase stability field, above the $\alpha+\gamma$ divariant loop; moreover, any experimental points at which α and γ phases coexist in equilibrium must fall along the calculated stability curves bounding the $\alpha+\gamma$ divariant loop.

This criterion of internal thermodynamic consistency can be of great utility when certain parameters in the thermodynamic model are unknown or poorly constrained. The appropriate procedure is simply to allow the uncertain thermodynamic parameter to vary within the bounds of its uncertainty until the computed phase diagram best matches the phase equilibrium data. Depending upon the complexity of the system under consideration and the number of variable parameters, this variation of parameters fitting procedure may be carried out by systematic trial and error or by a formal least squares inversion [*cf.* Gill et al., 1981, pp. 133-141]. In either case, it is important to perform a sensitivity analysis to determine how well this inversion procedure actually constrains the parameters and how sensitive the calculated phase diagram is to small changes in these parameters. (In general, the greater the number of parameters which must be determined in this manner, the more poorly constrained will be the individual parameters.) As an example, Bina and Wood [1984] used available phase equilibrium data to constrain the pressure dependence of the volume change of the eclogite to garnetite phase transition, since the bulk moduli of some of the garnetite phases were poorly constrained parameters. Conversely, the bulk moduli — and hence the pressure dependence of the volume change of phase transition — of the α-olivine and β-modified-spinel phases are well constrained. Bina and Wood [1987] used these parameters to tightly constrain the width (in pressure-composition space) of the $\alpha+\beta$ divariant stability loop, since this region of the phase diagram was poorly constrained by available phase equilibrium data.

Computing Stable Assemblages in Complex Systems

Now that we have both a formulation for the chemical potential of a component (equation (1)) and a set of thermodynamic data parameterizing internally consistent phase diagrams for numerous simple systems, we are ready to combine all of these data to calculate stable phase assemblages, mineral compositions, and associated

physical properties in complex multicomponent systems.

Phase Assemblages and Compositions

Given a system of arbitrary bulk chemical composition, we wish to determine which mineral phases can coexist at equilibrium at some pressure and temperature of interest, and we wish to know the equilibrium compositions of these stable phases. The equilibrium state of a system of fixed bulk composition is characterized by the minimum value of the Gibbs free energy of the system [*cf.* Denbigh, 1981, p. 83], namely:

$$G^{sys}_{P,T} = \sum_{\text{all } i,\phi} \overline{G}_i^{\phi}(P,T,X) n_i^{\phi} = \textit{minimum} \ ,$$

where $\overline{G}_i^{\phi}(P,T,X)$ is as in equation (2) and X is a function of the n_i^{ϕ}, the number of moles of component i in phase ϕ. For computational purposes, we may temporarily cease to distinguish between components and phases, instead counting each phase of a given component as a separate component. (*E.g.*, α–Mg_2SiO_4 and β–Mg_2SiO_4 will now be considered as distinct components.) Thus, for an N-component system, we have at equilibrium:

$$G^{sys}_{P,T} = \sum_{i=1}^{N} \overline{G}_i n_i = \textit{minimum} \ . \tag{6}$$

Here n_i is the number of moles of component i in the system, and $\overline{G}_i$ is the chemical potential of component i and is a function of pressure, temperature, and some subset of the n_j (*i.e.*, the n_j for those components j which were previously considered to be in the same phase as component i). Upon solving equation (6) at fixed pressure, temperature, and bulk composition, we obtain the n_i, namely the distribution and compositions of the stable equilibrium phases. Methods for solving equation (6) under these conditions are discussed in Appendix B.

Other Physical Properties

Given the composition of the stable phase assemblage at some pressure and temperature, in terms of either n_i or n_i^{ϕ}, it is a simple matter to compute the density of the assemblage:

$$\rho^{P,T} = \frac{\left\{ \sum_{\text{all } i,\phi} n_i^{\phi} M_i \right\}}{\left\{ \sum_{\text{all } i,\phi} n_i^{\phi} \, {}^{i\phi}\overline{V}_{P,T} \right\}} \ ,$$

where M_i is the molar mass (''gram formula weight'') of component i and the ${}^{i\phi}\overline{V}_{P,T}$ are the partial molar volumes from equation (2). Given the adiabatic bulk moduli ${}^{i\phi}K_S^{(1,T)}$ from equation (3), we may correct them for

pressure using a differentiated form of the Birch-Murnaghan equation (2):

$$ {}^{i\phi}K_S^{(P,T)} = {}^{i\phi}K_S^{(1,T)} \left[1 + 2f\right]^{\frac{5}{2}} \left[1 + 7f - 2\xi f \left[2 + 9f\right]\right] , $$

and compute the Voigt-Reuss-Hill (VRH) averaged aggregate bulk modulus [Watt, 1976]:

$$ {}^{sys}_{Voigt}K_S^{(P,T)} = \left[\sum_{all\ i,\phi} \frac{\omega_{i\phi}^{sys}}{{}^{i\phi}K_S^{(P,T)}} \right]^{-1} $$

$$ {}^{sys}_{Reuss}K_S^{(P,T)} = \sum_{all\ i,\phi} \omega_{i\phi}^{sys} \cdot {}^{i\phi}K_S^{(P,T)} , $$

so that:

$$ {}^{sys}_{VRH}K_S^{(P,T)} = \frac{1}{2} \left[{}^{sys}_{Voigt}K_S^{(P,T)} + {}^{sys}_{Reuss}K_S^{(P,T)} \right] , $$

where $\omega_{i\phi}^{sys}$ represents the volume fraction of phase ϕ of component i in the system:

$$ \omega_{i\phi}^{sys} = \frac{{}^{i\phi}\bar{V}_{P,T}}{\left[\sum_{all\ i,\phi} n_i^{\phi}\ {}^{i\phi}\bar{V}_{P,T} \right]} . $$

It is now a simple matter to calculate the bulk sound velocity $\sqrt{\bar{\Phi}}$, since the seismic parameter Φ is given by:

$$ \Phi = \frac{{}^{sys}K_S}{{}^{sys}\rho} . $$

This may be directly compared to observed seismic profiles, given complimentary P- and S-wave velocity data (V_P and V_S, respectively), since:

$$ \Phi = (V_P)^2 - \frac{4}{3}(V_S)^2 . $$

If, on the other hand, we wish to predict independent P- and S-wave velocities for our model system, we require data regarding the shear moduli ${}^{i\phi}\mu$ of the various components, since:

$$ (V_P)^2 = \frac{{}^{sys}K_S - \frac{4}{3}{}^{sys}\mu}{{}^{sys}\rho} $$

$$ (V_S)^2 = \frac{{}^{sys}\mu}{{}^{sys}\rho} , $$

where, as for the bulk modulus ${}^{sys}K_S$, we have:

$$ {}^{sys}_{VRH}\mu^{P,T} = \frac{1}{2} \left[\left[\sum_{all\ i,\phi} \frac{\omega_{i\phi}^{sys}}{{}^{i\phi}\mu^{(P,T)}} \right]^{-1} + \sum_{all\ i,\phi} \omega_{i\phi}^{sys} \cdot {}^{i\phi}\mu^{(P,T)} \right] . \qquad (7) $$

Thus, in order to compute the aggregate shear modulus from equation (7), we require knowledge of the shear moduli of all of the components in all of the phases at 1 bar and some reference temperature T_0, as well as their

pressure and temperature derivatives [*cf.* Bina and Wood, 1987], namely:

$$ {}^{i\phi}\mu^{P,T} = {}^{i\phi}\mu^{P,T_0} + \int_{T_0}^{T} \left(\frac{\partial {}^{i\phi}\mu}{\partial \hat{T}} \right)_P d\hat{T} + \int_{1}^{P} \left(\frac{\partial {}^{i\phi}\mu}{\partial \hat{P}} \right)_T d\hat{P} \ . $$

Thus, to compute independent P- and S-wave velocities for, say, an N-component/phase system requires 3N additional parameters — a shear modulus and two derivatives for each component/phase. As these additional parameters play no role in the thermodynamic formalism applied earlier to obtain an internally consistent data set, poorly known values cannot be further constrained by independent phase equilibrium observations. Thus, unless unusually good data on the pressure and temperature dependence of the shear moduli are available, such computation of individual P- and S-wave velocities is subject to considerably greater uncertainty than the computation of the bulk sound velocity $\sqrt{\Phi}$.

Application to the Upper Mantle

As mentioned above, Bina and Wood [1984] computed internally consistent high pressure phase diagrams for the simple systems $Mg_4Si_4O_{12}$-$Mg_3Al_2Si_3O_{12}$, $Fe_4Si_4O_{12}$-$Fe_3Al_2Si_3O_{12}$, and $Ca_2Mg_2Si_4O_{12}$-$Ca_{1.5}Mg_{1.5}Al_2Si_3O_{12}$. Using a free energy minimization approach, they showed that the eclogite to garnetite transition — the dissolution of pyroxene into the garnet phase to form a garnet-majorite solid solution — occurs gradually over a broad depth interval and would produce no sharp increase in seismic velocity such as that observed in the earth at 400 km depth. Bina and Wood [1987] determined an internally consistent high pressure phase diagram for the Mg_2SiO_4-Fe_2SiO_4 join and demonstrated that the α-olivine to β-modified-spinel transition would occur over a sufficiently small depth interval to produce a sharp seismic discontinuity such as that at 400 km. They concluded, as did Weidner [1985], that observed seismic velocities in the upper mantle of the earth are consistent with an upper mantle of a uniform olivine-rich, or peridotitic, bulk composition. In this section we expand upon this previous work by incorporating more recent experimental results into the internally consistent thermodynamic data set. We then use this data set to compute seismic velocity profiles for a suite of upper mantle models ranging from eclogite to pure olivine in bulk composition.

Thermodynamic Data

For this analysis, we made use of the thermodynamic data set for low pressure phases of Wood and Holloway [1984]. To this we added the recent data of Kandelin and Weidner [1984] for jadeite and that of Duffy and Vaughan [1986] for enstatite. For the α, β, and γ phases of olivine, we adopted the data set of Bina and Wood [1987]. For the quartz, coesite, and stishovite phases of SiO_2, we used the data of Holm et al. [1967] and Jeanloz and Thompson [1983]. Finally, for the high pressure majorite components of the garnet phase, we made use of the thermodynamic analysis of Bina and Wood [1984], modified in the manner described below.

Bina and Wood [1984] derived an internally consistent thermodynamic data set for the transition:

$$\underset{\text{pyroxene}}{M_4Si_4O_{12}} = \underset{\text{garnet}}{M_4Si_4O_{12}}, \quad M \in \{Mg, Fe, Ca_{0.5}Mg_{0.5}\},$$

using the phase equilibrium data of Akaogi and Akimoto [1977] and Akaogi [1978]. However, recent work by Akaogi et al. [1987] has shown that the pressure calibration used in these phase equilibrium studies in subject to considerable error. Akaogi et al. [1987], using numerous recent pressure calibration data, have produced a revised pressure scale for the experiments in the $Mg_4Si_4O_{12}$-$Mg_3Al_2Si_3O_{12}$ system. We have applied their pressure correction to the $Fe_4Si_4O_{12}$-$Fe_3Al_2Si_3O_{12}$ and $Ca_2Mg_2Si_4O_{12}$-$Ca_{1.5}Mg_{1.5}Al_2Si_3O_{12}$ data as well. These recalibrated data points are shown by the polygonal symbols in Figures 1 and 2. (Note that these are synthesis data and have not rigorously demonstrated equilibrium by the criterion of ''reversibility'' [*cf.* Fyfe, 1960].)

In addition, Akaogi et al. [1987] used an *in situ* synchrotron technique to determine the bulk modulus of $Mg_4Si_4O_{12}$ majorite. Bina and Wood [1984] made use of the majorite bulk modulus data of Jeanloz [1981]. However, these data may be subject to considerable error since they give majorite bulk moduli which are larger than the moduli of the corresponding aluminous garnets, while simple crystallochemical arguments [D. Weidner, pers. comm.; Akaogi et al., 1987] suggest that they should be smaller. The new data of Akaogi et al. [1987] do, in fact, yield values for the majorite components which are smaller than those for their aluminous counterparts. Akaogi et al. [1987] performed bulk modulus measurements on samples of two garnets — one of composition 100% pyrope and the other of 42% pyrope with 58% Mg-majorite — and extrapolated their results linearly to a pure Mg-majorite endmember. Since their values for pure pyrope differ from the established value [Jeanloz and Thompson, 1983; Levien et al., 1979] by 0.06 Mbar, we have corrected their Mg-majorite value for systematic error by the same amount. Finally, Akaogi et al. [1987] measured bulk moduli for Mg-majorite only. We have estimated values for the Fe- and CaMg-garnets by assuming the relationship:

$$\frac{K_S^{Mg_4Si_4O_{12}(gt)}}{K_S^{Mg_3Al_2Si_3O_{12}(gt)}} = \frac{K_S^{Fe_4Si_4O_{12}(gt)}}{K_S^{Fe_3Al_2Si_3O_{12}(gt)}} = \frac{K_S^{Ca_2Mg_2Si_4O_{12}(gt)}}{K_S^{Ca_{1.5}Mg_{1.5}Al_2Si_3O_{12}(gt)}} ,$$

giving the bulk modulus values shown in Table 1. Using this revised data, we have calculated the internally consistent phase diagrams for the eclogite-garnetite transition shown in Figures 1 and 2.

Results

Using the internally consistent thermodynamic data set described above, we have applied the technique of free energy minimization and calculated stable phase assemblages and their corresponding seismic velocities under upper mantle conditions for five model mantle bulk compositions: an eclogite (a natural alkali olivine basalt from Green and Ringwood [1967]), a ''piclogite'' (a model from Anderson and Bass [1986]), a pyrolite (model Pyrolite III from Ringwood [1975]), a peridotite (a natural Lizard peridotite from Ringwood [1975]), and pure olivine ($Fo_{90}Fa_{10}$). These models represent a range of bulk composition from olivine-free eclogite at one extreme to 100% olivine at the other; the low pressure mineralogies of these model compositions are given in Table 2. Calculated bulk sound velocities for these five compositions are given in Figure 3 along 1700 K and 2000 K isotherms for pressures corresponding to those in the transition zone, and the reference seismic model GCA+TNA [*cf.* Bina and Wood, 1987; Walck, 1984; Grand and Helmberger, 1984] is shown for comparison. Clearly the olivine-poor compositions are unsatisfactory: the eclogite exhibits no 400 km seismic discontinuity, and the magnitude of the 400 km discontinuity computed for the piclogite model is far smaller than that actually observed in the earth. Seismic velocities for the pyrolite are in much better agreement with the observed velocities, but the calculated 400 km discontinuity for this composition is still too small. The size of the 400 km discontinuity computed for the pure olivine composition is somewhat larger than observed seismically. The best-fit model bulk composition for the upper mantle appears to be a few more percent enriched in olivine than the peridotite (at 74% olivine).

Conclusions

In summary, available thermodynamic data may be combined with data from phase equilibrium experiments to produce internally consistent phase diagrams for simple systems, with the well-constrained features of one data set placing constraints upon the more poorly-determined features of the other data set. The internally con-

sistent thermodynamic and thermoelastic data set which parameterizes these phase diagrams may then be used to calculate stable phase assemblages and associated elastic properties (such as seismic velocities) as functions of pressure and temperature for model bulk chemical compositions using the technique of free energy minimization. Here we have computed seismic velocities for a variety of model upper mantle bulk compositions ranging from eclogite to pure olivine. Upon comparison with observed transition zone seismic velocities, we conclude that a peridotitic bulk composition (~75% olivine) is consistent with upper mantle seismic velocities and is required to generate a 400 km discontinuity of appropriate sharpness and magnitude. We find no evidence for chemical stratification in the mantle at depths shallower than 650 km [*e.g.*, Anderson and Bass, 1986].

Acknowledgments. We thank Alexandra Navrotsky for providing us with a preprint of Akaogi et al. [1987]; we thank George Helffrich, Emile Okal, and Seth Stein for numerous helpful discussions. This material is based upon work supported under a National Science Foundation Graduate Fellowship (C.R.B.) and National Science Foundation grant EAR-8416793 (B.J.W.).

REFERENCES

Akaogi, M., High-pressure phase equilibria of the mantle minerals and mineralogical constitution of the mantle transition zone, Ph. D. dissertation, University of Tokyo, Tokyo, 1978.

Akaogi, M., and S. Akimoto, Pyroxene-garnet solid-solution equilibria in the systems Mg Si O -Mg Al Si O and Fe Si O -Fe Al Si O at high pressures and temperatures, *Phys. Earth Planet. Inter.*, 90-106, 1977.

Akaogi, M., A. Navrotsky, T. Yagi, and S. Akimoto, Pyroxene-garnet transformation: thermochemistry and elasticity of garnet solid solutions, and application to mantle models, *in prep.*, 1987.

Albutt, T. C., *Science and Medieval Thought*, 1901.

Anderson, D. L., and J. D. Bass, Transition region of the Earth's upper mantle, *Nature, 320*, 321-328, 1986.

Ashcroft, N. W., and N. D. Mermin, *Solid State Physics*, 826 pp., Holt, Rinehart and Winston, Philadelphia, 1976.

Bernal, J. D., Discussion, *Observatory, 59*, 268, 1936.

Bina, C. R., and B. J. Wood, The eclogite to garnetite transition — experimental and thermodynamic constraints, *Geophys. Res. Lett., 11*, 955-958, 1984.

Bina, C. R., and B. J. Wood, The 400 km seismic discontinuity and the proportion of olivine in the Earth's upper mantle, *Nature, 324*, 449-451, 1986.

Bina, C. R., and B. J. Wood, The olivine-spinel transitions: experimental and thermodynamic constraints and implications for the nature of the 400 km seismic discontinuity, *J. Geophys. Res., 92*, 4853-4866, 1987.

Birch, F., Elasticity and constitution of the Earth's interior, *J. Geophys. Res., 57*, 227-286, 1952.

Bullen, K. E., The variation of density and the ellipticities of strata of equal density within the earth, *Mon. Not. R. astron. Soc., Geophys. Suppl., 3*, 395-401, 1936.

Davidon, W. C., Variable metric methods for minimization, A. E. C. Res. and Develop. Report ANL-5990, Argonne National Laboratory, Argonne, Illinois, 1959.

Denbigh, K., *The Principles of Chemical Equilibrium*, 494 pp., Cambridge University Press, Cambridge, 1981.

Duffy, T. S. and M. T. Vaughan, Elasticity of enstatite by Brillouin scattering, *EOS Trans. Amer. Geophys. Union, 67*, 374, 1986.

Fisher, G. W., and L. G. Medaris, Jr., Cell dimensions and x-ray determinative curve for synthetic Mg-Fe olivines, *Am. Mineral., 54*, 741-753, 1969.

Fletcher, R., and M. J. D. Powell, A rapidly convergent descent method for minimization, *Computer Journal, 6*, 163-168, 1963.

Fyfe, W. S., Hydrothermal synthesis and determination of equilibrium between minerals in the subsolidus region, *J. Geol., 68*, 553-556, 1960.

Gerald, C. F., and P. O. Wheatley, *Applied Numerical Analysis*, 579 pp., Addison-Wesley Publishing Company, Inc., Reading, Massachusetts, 1984.

Gill, P. E., W. Murray, and M. H. Wright, *Practical Optimization*, 401 pp., Academic Press, London, 1981.

Grand, S. P., and D. V. Helmberger, Upper mantle shear structure of North America, *Geophys. J. R. astron. Soc., 76*, 399-438, 1984.

Green, D. H., and A. E. Ringwood, An experimental investigation of the gabbro to eclogite transformation and its petrological applications, *Geochim. et Cosmochim. Acta, 31*, 767-833, 1967.

Hamilton, Sir William, *Lectures on Metaphysics, Volume II*, 1837.

Haselton, H. T., and R. C. Newton, Thermodynamics of pyrope-grossular garnets and their stabilities at high temperatures and high pressures, *J. Geophys. Res. 85*, 6973-6982, 1980.

Holm, J. L., O. J. Kleppa, and E. F. Westrum, Jr., Thermodynamics of polymorphic transformations in silica. Thermal properties from 5 to 1070°K and P-T stability fields for coesite and stishovite. *Geochim. et Cosmochim. Acta, 31*, 2289-2307, 1967.

Hurley, J. F., *Intermediate Calculus: Multivariable Functions and Differential Equations with Applications*, 726 pp., Saunders College, Philadelphia, 1980.

Jeanloz, R., Majorite: vibrational and compressional properties of a high-pressure phase, *J. Geophys. Res., 86*, 6171-6179, 1981.

Jeanloz, R., and A. B. Thompson, Phase transitions and mantle discontinuities, *Rev. Geophys. Space Phys., 21*, 51-74, 1983.

Kandelin, J. and D. J. Weidner, Elasticity of jadeite, *EOS Trans. Amer. Geophys. Union, 65*, 1105-1106, 1984.

Levien, L., C. T. Prewitt, and D. J. Weidner, Compression of pyrope, *Am. Mineral., 64*, 805-808, 1979.

Ringwood, A. E., *Composition and Petrology of the Earth's Mantle*, 618 pp., McGraw-Hill Book Company, New York, 1975.

Storey, S. H., and F. Van Zeggeren, Computation of chemical equilibrium compositions, *Can. J. Chem. Eng., 42*, 54-55, 1964.

Walck, M. C., The P-wave upper mantle structure beneath an active spreading center: the Gulf of California, *Geophys. J. R. astron. Soc., 76*, 697-723, 1984.

Watt, J. P., G. F. Davies, and R. J. O'Connell, The elastic properties of composite materials, *Rev. Geophys. Space Phys., 14*, 541-563, 1976.

Weidner, D. J., A mineral physics test of a pyrolite mantle, *Geophys. Res. Lett., 12*, 417-420, 1985.

Wood, B. J., and J. R. Holloway, Theoretical prediction of phase relationships in planetary mantles, *J. Geophys. Res., 87 Supplement*, A19-A30, 1982.

Wood, B. J., and J. R. Holloway, A thermodynamic model for subsolidus equilibria in the system CaO-MgO-Al_2O_3-SiO_2, *Geochim. Cosmochim. Acta, 48*, 159-176, 1984.

Wood, B. J., and O. J. Kleppa, Thermochemistry of forsterite-fayalite olivine solutions, *Geochim. Cosmochim. Acta, 45*, 529-534, 1981.

APPENDIX A: CALCULATION OF DIVARIANT PHASE RELATIONS

The system of equilibrium conditions in the divariant region $\alpha+\beta$ consists of equations (*cf.* equation (2-3)) of the form:

$$\begin{cases} \overline{G}^{\alpha}_{Mg_2SiO_4} = \overline{G}^{\beta}_{Mg_2SiO_4} \\ \overline{G}^{\alpha}_{Fe_2SiO_4} = \overline{G}^{\beta}_{Fe_2SiO_4} \ . \end{cases}$$

We may define difference functions, F, such that:

$$F_i^{\alpha\beta} \equiv \overline{G}_i^{\alpha} - \overline{G}_i^{\beta} \ ,$$

for each component i, and we may then seek solutions to equations of the form:

$$F_i^{\alpha\beta}\left[X_1^{\alpha},\ X_1^{\beta},\ P,\ T\right] = 0 \ .$$

In the divariant region, the requisite system of equations is simply:

$$\begin{cases} F_1^{\alpha\beta}\left[X_1^{\alpha},\ X_1^{\beta},\ P,\ T\right] = 0 \\ F_2^{\alpha\beta}\left[X_1^{\alpha},\ X_1^{\beta},\ P,\ T\right] = 0 \ . \end{cases}$$

Where $X_2^{\phi} = 1 - X_1^{\phi}$ for any given phase ϕ.

To solve for the case of equilibrium involving all three phases α, β, and γ, we need only include two more equations — those involving either the α-γ or the β-γ difference functions — in this system.

In order to solve the system, we may employ Newton's method [*cf.* Gerald and Wheatley, 1984, pp. 133-139] to reduce the solution of the system of non-linear equations to iterations of solutions of systems of linear equations. We accomplish this by developing the first-order (*i.e.*, linear) Taylor series approximation [*cf.* Hurley, 1980, pp. 710-714] to each function F_i, so that:

$$\begin{cases} 0 \approx \left[F_1^{\alpha\beta}\right] + \left[\dfrac{\partial F_1^{\alpha\beta}}{\partial X_1^{\alpha}}\right] \cdot \left[X_{1,new}^{\alpha} - X_{1,old}^{\alpha}\right] + \left[\dfrac{\partial F_1^{\alpha\beta}}{\partial X_1^{\beta}}\right] \cdot \left[X_{1,new}^{\beta} - X_{1,old}^{\beta}\right] \\ 0 \approx \left[F_2^{\alpha\beta}\right] + \left[\dfrac{\partial F_2^{\alpha\beta}}{\partial X_1^{\alpha}}\right] \cdot \left[X_{1,new}^{\alpha} - X_{1,old}^{\alpha}\right] + \left[\dfrac{\partial F_2^{\alpha\beta}}{\partial X_1^{\beta}}\right] \cdot \left[X_{1,new}^{\beta} - X_{1,old}^{\beta}\right] \ , \end{cases} \qquad \text{(A-1)}$$

where each function F_i and its derivatives are evaluated at the appropriate approximate root $X_{1,old}^{\phi}$.

We may use forward finite differences [*cf.* Gerald and Wheatley, 1984, pp. 233-238] for the calculation of derivatives, so that:

$$\begin{cases} \left(\dfrac{\partial F_i^{\alpha\beta}}{\partial X_1^{\alpha}}\right)_{P,T,X_{1,old}^{\beta}} \approx \dfrac{F_i^{\alpha\beta}\left(X_{1,old}^{\alpha}+\delta,\ X_{1,old}^{\beta},\ P,\ T\right) - F_i^{\alpha\beta}\left(X_{1,old}^{\alpha},\ X_{1,old}^{\beta},\ P,\ T\right)}{\delta} \\ \left(\dfrac{\partial F_i^{\alpha\beta}}{\partial X_1^{\beta}}\right)_{P,T,X_{1,old}^{\alpha}} \approx \dfrac{F_i^{\alpha\beta}\left(X_{1,old}^{\alpha},\ X_{1,old}^{\beta}+\delta,\ P,\ T\right) - F_i^{\alpha\beta}\left(X_{1,old}^{\alpha},\ X_{1,old}^{\beta},\ P,\ T\right)}{\delta} \end{cases},$$

where δ is some small finite perturbation parameter.

The linear systems (A-1) may be solved by a matrix method, such as Gaussian elimination employing partial pivoting [*cf.* Gerald and Wheatley, 1984, pp. 88-95]. Each solution of a system such as (A-1) will give the correction factors $(X_{1,new}^{\phi} - X_{1,old}^{\phi})$ by which the previous approximate solution $X_{1,old}^{\phi}$ must be modified, and hence values for $X_{1,new}^{\phi}$ may be obtained for all pertinent phases ϕ. These corrections may be applied iteratively until the absolute differences between consecutive solutions fall below some arbitrary tolerance value. Note that, when solving the univariant problem for three coexisting phases numerically, it may be necessary to scale the pressure variable to the same order of magnitude as the composition (mole fraction) variables (*i.e.*, order 10^{-1}) in order to avoid forming a nearly singular matrix during linearization.

Initial estimates of the solution variables for Newton's method may be obtained as follows. The partial molar free energy of Mg_2SiO_4 in the α phase is given by:

$$\bar{G}_{Mg_2SiO_4}^{\alpha} = G_{Mg_2SiO_4}^{\alpha}(T) + \int_1^P V_{Mg_2SiO_4}^{\alpha} dP' + RT \ln a_{Mg_2SiO_4}^{\alpha} . \qquad \text{(A-2)}$$

In equation (A-2), $G_{Mg_2SiO_4,T}^{\alpha}$ refers to the free energy of pure Mg_2SiO_4 in the α phase at temperature T and 1 bar. Equilibrium between α and β phases gives the conditions:

$$\begin{cases} \bar{G}_{Mg_2SiO_4}^{\beta} - \bar{G}_{Mg_2SiO_4}^{\alpha} = \Delta G_{Mg_2SiO_4}^{\alpha\rightarrow\beta} = 0 \\ \bar{G}_{Fe_2SiO_4}^{\beta} - \bar{G}_{Fe_2SiO_4}^{\alpha} = \Delta G_{Fe_2SiO_4}^{\alpha\rightarrow\beta} = 0 . \end{cases}$$

Upon constructing equations similar to (A-2) for the β phase and for the Fe_2SiO_4 components, the above may be expanded to give:

$$\begin{cases} \Delta G^{\alpha,\beta}_{Mg_2SiO_4} = \Delta G^{\alpha,\beta}_{Mg_2SiO_4}(T) + \int_1^P \Delta V^{\alpha,\beta}_{Mg_2SiO_4} dP' + RT \ln \kappa^{\alpha\to\beta}_{Mg_2SiO_4} = 0 \\ \Delta G^{\alpha,\beta}_{Fe_2SiO_4} = \Delta G^{\alpha,\beta}_{Fe_2SiO_4}(T) + \int_1^P \Delta V^{\alpha,\beta}_{Fe_2SiO_4} dP' + RT \ln \kappa^{\alpha\to\beta}_{Fe_2SiO_4} = 0 \ , \end{cases} \tag{A-3}$$

where the equilibrium constants (the $\kappa_i^{\alpha\to\beta}$'s) are given by:

$$\begin{cases} \kappa^{\alpha\to\beta}_{Mg_2SiO_4} \equiv \dfrac{a^{\beta}_{Mg_2SiO_4}}{a^{\alpha}_{Mg_2SiO_4}} \\ \kappa^{\alpha\to\beta}_{Fe_2SiO_4} \equiv \dfrac{a^{\beta}_{Fe_2SiO_4}}{a^{\alpha}_{Fe_2SiO_4}} \ . \end{cases}$$

We may begin by assuming an ideal single-site binary solid solution (*i.e.*, $a_i^{\phi} = X_i^{\phi}$), so that:

$$\begin{cases} \kappa^{\alpha\to\beta}_{Mg_2SiO_4} = \dfrac{X^{\beta}_{Mg_2SiO_4}}{X^{\alpha}_{Mg_2SiO_4}} \\ \kappa^{\alpha\to\beta}_{Fe_2SiO_4} = \dfrac{X^{\beta}_{Fe_2SiO_4}}{X^{\alpha}_{Fe_2SiO_4}} = \dfrac{1-X^{\beta}_{Mg_2SiO_4}}{1-X^{\alpha}_{Mg_2SiO_4}} \ . \end{cases}$$

Upon solving these two equations in two unknowns (the $X^{\phi}_{Mg_2SiO_4}$'s), we obtain:

$$\begin{cases} X^{\alpha}_{Mg_2SiO_4} = \dfrac{\kappa^{\alpha\beta}_{Fe_2SiO_4} - 1}{\kappa^{\alpha\beta}_{Fe_2SiO_4} - \kappa^{\alpha\beta}_{Mg_2SiO_4}} \\ X^{\beta}_{Mg_2SiO_4} = X^{\alpha}_{Mg_2SiO_4} \cdot \kappa^{\alpha\beta}_{Mg_2SiO_4} \ . \end{cases} \tag{A-4}$$

We may now solve the two equations (A-3) simultaneously for the two unknown equilibrium constants (the $\kappa_i^{\alpha\to\beta}$'s) and insert these values into equations (A-4) to obtain our initial compositional estimate.

This estimation process is easily extended to four equations in four unknowns, for approximation to the solution of the case of univariant equilibrium involving all three phases, by the inclusion of suitable expressions involving $\kappa_i^{\alpha\to\gamma}$.

APPENDIX B: MINIMIZATION OF FREE ENERGY

The problem of free energy minimization is to determine the relative amounts of a set of components which define the minimum value of the Gibbs free energy of the system at a pressure and temperature of interest and a fixed bulk chemical composition. Here we examine a steepest descent method [*cf.* Storey and Van Zeggeren, 1964], which utilizes only first order derivatives, and a quasi-Newton method [*cf.* Gill et al., 1981, pp. 116-125], which utilizes second order derivatives, for computing the minimum of the Gibbs free energy function subject to the constraint of constant bulk composition. Finally, we discuss the relative practical utility of these two methods.

Steepest Descent Method

The problem is to minimize the free energy G of the system under consideration in terms of the chemical potentials $\overline{G}_i$ and amounts n_i of the N components i comprising the system, namely:

$$G \equiv \sum_{i=1}^{N} \overline{G}_i n_i = \textit{minimum} \ . \tag{B-1}$$

The constraint of constant bulk chemical composition may be formulated in terms of the mass balance conditions:

$$\sum_{i=1}^{N} a_{ji} n_i = Y_j \ , \quad j=1, \cdots ,M \ . \tag{B-2}$$

Here we have fixed the bulk composition in terms of the fundamental oxides in the system; a_{ji} is the number of moles of oxide j in one mole of component i, and Y_j is the total number of moles of oxide j in the system. Upon introducing a search parameter λ, the differential forms of equations (B-1) and (B-2) become:

$$\frac{dG}{d\lambda} = \sum_{i=1}^{N} \overline{G}_i \frac{dn_i}{d\lambda} \ , \tag{B-3}$$

subject to:

$$\sum_{i=1}^{N} a_{ji} \frac{dn_i}{d\lambda} = 0 \ , \quad j=1, \cdots ,M \ , \tag{B-4}$$

where we have used the Gibbs-Duhem equation [*cf.* Denbigh, 1981, p. 93] at constant pressure and temperature:

$$dG = \sum_{i=1}^{N} \overline{G}_i dn_i \ ,$$

in the differentiation of equation (B-1). In order to prevent the n_i from assuming nonphysical negative values, we adopt the change of variables:

$$n_i \equiv \exp(\eta_i) \ .$$

Hence, the equations (B-3) and (B-4) become:

$$\begin{cases} \dfrac{dG}{d\lambda} = \sum\limits_{i=1}^{N} \bar{G}_i n_i \dfrac{d\eta_i}{d\lambda} \\ \sum\limits_{i=1}^{N} a_{ji} n_i \dfrac{d\eta_i}{d\lambda} = 0 \ , \quad j=1, \cdots ,M \ . \end{cases}$$

At any given composition $\{n'_i\}_1^N$ (given by the values η'_i), we find the direction of steepest descent by determining the N values of the $\dfrac{d\eta_i}{d\lambda}$ for which $\dfrac{dG}{d\lambda}$ is an extremum. Upon introducing an additional normalization condition, our problem becomes:

$$\begin{cases} \dfrac{dG}{d\lambda} = \sum\limits_{i=1}^{N} \bar{G}'_i n'_i \dfrac{d\eta_i}{d\lambda} = \textit{extremum} \\ \sum\limits_{i=1}^{N} a_{ji} n'_i \dfrac{d\eta_i}{d\lambda} = 0 \ , \quad j=1, \cdots ,M \\ \sum\limits_{i=1}^{N} \left\{ \dfrac{d\eta_i}{d\lambda} \right\}^2 = 1 \ , \end{cases} \tag{B-5}$$

where the $\bar{G}'_i$ represent the chemical potentials of the N components at the composition $\{n'_i\}_1^N$. Applying the method of Lagrange multipliers [*cf.* Hurley, 1980, pp. 223-228], we obtain:

$$\sum_{i=1}^{N} \bar{G}'_i n'_i \frac{d^2\eta_i}{d\lambda^2} - 2\nu \sum_{i=1}^{N} \left\{ \frac{d\eta_i}{d\lambda} \right\} \frac{d^2\eta_i}{d\lambda^2} - \sum_{j=1}^{M} \left\{ \xi_j \sum_{i=1}^{N} a_{ji} n'_i \frac{d^2\eta_i}{d\lambda^2} \right\} = 0 \ ,$$

for the M+1 Lagrange multipliers ν and ξ_j. We are solving for the N values of $\dfrac{d\eta_i}{d\lambda}$ at the composition $\{n'_i\}_1^N$; the $\dfrac{d^2\eta_i}{d\lambda^2}$ may take on any arbitrary values; hence we have:

$$\bar{G}'_i n'_i - 2\nu \frac{d\eta_i}{d\lambda} - \sum_{j=1}^{M} \xi_j a_{ji} n'_i = 0 \ , \quad i=1, \cdots ,N \ . \tag{B-6}$$

Upon multiplying by $a_{ki} n'_i$, summing over all N components i, and applying the mass balance condition (B-4), we arrive at:

$$\sum_{j=1}^{M}\left[\sum_{i=1}^{N}a_{ki}a_{ji}\left(n'_i\right)^2\right]\xi_j = \sum_{i=1}^{N}\bar{G}'_i a_{ki}\left(n'_i\right)^2 , \quad k=1, \cdots ,M .$$

We may solve this system of M linear equations for the M unknown values of the ξ_j using such standard techniques as Gaussian elimination with partial pivoting [*cf.* Gerald and Wheatley, 1984, pp. 88-95], and from equation (B-6) we have:

$$\frac{d\eta_i}{d\lambda} = \frac{n'_i}{2\nu}\left[\bar{G}'_i - \sum_{j=1}^{M}\xi_j a_{ji}\right] , \quad i=1, \cdots ,N ,$$

where ν is chosen to satisfy the normalization condition comprising the third of equations (B-5). We now repeat the above procedure, obtaining our new composition $\{\hat{n}_i\}_1^N$ from the values of $\hat{\eta}_i$ given by:

$$\hat{\eta}_i = \eta'_i + \left(\frac{d\eta_i}{d\lambda}\right)\Delta\lambda , \quad i=1, \cdots ,N ,$$

where the sign and magnitude of $\Delta\lambda$ are chosen by an accurate line search technique [*cf.* Gill et al., 1981, pp. 100-102] so as to produce a sufficient decrease in the free energy G.

This procedure may be repeated iteratively until no further sufficient decrease in the free energy G can be achieved with suitable variations in composition. In practice, it is often useful to impose the mass-balance constraints (B-2) at every iteration to prevent the compositional drift which attends the use of finite values of $\Delta\lambda$.

Quasi-Newton Method

The problem is to find the compositions $\mathbf{n}_i$ at which the free energy G of the system attains a minimum:

$$G(\mathbf{n}) \equiv \bar{\mathbf{G}}^T\mathbf{n} = \textit{minimum} , \tag{B-7}$$

subject to constant bulk composition formulated in terms of the mass balance constraints:

$$\mathbf{c}(\mathbf{n}) \equiv A\,\mathbf{n} - \mathbf{y} = 0 . \tag{B-8}$$

Here $\bar{\mathbf{G}}$ and $\mathbf{n}$ are N-element vectors whose *i*th elements are the chemical potential and number of moles, respectively, of component i; $\mathbf{y}$ is an M-element vector whose *j*th element is the total number of moles of oxide j in the system, and A is an M×N matrix whose *ij*th element is the number of moles of oxide j in one mole of component i. In order to ensure that the compositions $\mathbf{n}_i$ do not take on nonphysical negative values, we adopt the change of variables:

$$\mathbf{n}_i \equiv \exp(\boldsymbol{\eta}_i) .$$

We now introduce a quadratic penalty function formulation [*cf.* Gill et al., 1981, p. 208], transforming equations

(B-7) and (B-8) into:

$$f(\boldsymbol{\eta}) \equiv G(\boldsymbol{\eta}) - \theta \mathbf{c}(\boldsymbol{\eta})^T \mathbf{c}(\boldsymbol{\eta}) = \textit{minimum} \ , \tag{B-9}$$

where θ is some scalar penalty parameter. Given an initial estimate of the composition $\boldsymbol{\eta}'$, we expand our new objective function $f(\boldsymbol{\eta})$ in a second order Taylor series [*cf.* Hurley, 1980, pp. 710-714] about $\boldsymbol{\eta}'$:

$$f(\boldsymbol{\eta}) \approx f(\boldsymbol{\eta}') + \mathbf{g}^T \left[\boldsymbol{\eta} - \boldsymbol{\eta}'\right] + \frac{1}{2} \left[\boldsymbol{\eta} - \boldsymbol{\eta}'\right]^T H \left[\boldsymbol{\eta} - \boldsymbol{\eta}'\right] .$$

Here $\mathbf{g}$ is the gradient vector evaluated at $\boldsymbol{\eta} = \boldsymbol{\eta}'$:

$$\mathbf{g} \equiv \nabla f \Big|_{\boldsymbol{\eta}'} ,$$

and H is the symmetric N×N Hessian matrix such that:

$$H_{ij} \equiv \frac{\partial^2 \mathbf{f}}{\partial \boldsymbol{\eta}_i \partial \boldsymbol{\eta}_j} \Bigg|_{\boldsymbol{\eta}'} .$$

Now if H is positive definite [*cf.* Gill et al., 1981, p. 25], then the minimum of $f(\boldsymbol{\eta})$ is given by:

$$\nabla f \approx \mathbf{g} + \left[\boldsymbol{\eta} - \boldsymbol{\eta}'\right] H = 0 \ , \tag{B-10}$$

so that we may obtain our next compositional estimate $\hat{\boldsymbol{\eta}}$ from:

$$\hat{\boldsymbol{\eta}} = \boldsymbol{\eta}' - \varepsilon H^{-1} \mathbf{g} \ , \tag{B-11}$$

where ε is chosen by line search [*cf.* Gill et al., 1981, 100-102] so as to produce a sufficient decrease in $f(\boldsymbol{\eta})$. While we may compute the gradient vector $\mathbf{g}$ at each iteration by a finite difference method [*cf.* Gerald and Wheatley, 1984, pp. 233-238], the determination of the inverse Hessian matrix H^{-1} at each iteration is an imposing computational problem. We proceed by beginning with an initial estimate Q for H^{-1}, the identity matrix I for example, and updating the second order information in Q at each iteration. Our new compositional estimate $\hat{\boldsymbol{\eta}}$ from equation (B-11) now becomes:

$$\hat{\boldsymbol{\eta}} = \boldsymbol{\eta}' - \varepsilon Q \mathbf{g} \ .$$

Since, from equation (B-10), we have that:

$$H^{-1} \left[\nabla f \Big|_{\hat{\boldsymbol{\eta}}} - \mathbf{g} \right] \approx \hat{\boldsymbol{\eta}} - \boldsymbol{\eta}' \ , \tag{B-12}$$

we correct Q for the next iteration by an ''update matrix'' D, namely:

$$\hat{Q} = Q + D \ ,$$

such that $\hat{Q}$ also satisfies condition (B-12):

$$\hat{Q}\left(\nabla f\Big|_{\hat{\boldsymbol{\eta}}} - \mathbf{g}\right) = \hat{\boldsymbol{\eta}} - \boldsymbol{\eta}' \ .$$

From the numerous possible choices [*cf.* Gill et al., 1981, pp. 117-120] for the form of D, we have chosen the Davidon-Fletcher-Powell (DFP) [Davidon, 1959; Fletcher and Powell, 1963] update formula:

$$D = \frac{\mathbf{r}\mathbf{r}^{\mathrm{T}}}{\mathbf{r}^{\mathrm{T}}\mathbf{z}} - \frac{Q\mathbf{z}\mathbf{z}^{\mathrm{T}}Q}{\mathbf{z}^{\mathrm{T}}Q\mathbf{z}} \ ,$$

where:

$$\mathbf{r} \equiv \hat{\boldsymbol{\eta}} - \boldsymbol{\eta}'$$
$$\mathbf{z} \equiv \nabla f\Big|_{\hat{\boldsymbol{\eta}}} - \nabla f\Big|_{\boldsymbol{\eta}'} = \hat{\mathbf{g}} - \mathbf{g} \ .$$

This DFP update has the property that if the initial approximation to the inverse Hessian Q is positive definite, then all subsequent updated estimates $\hat{Q}$ are also positive definite.

This procedure may be repeated iteratively until no further sufficient decrease in the objective function $f(\boldsymbol{\eta})$ can be achieved with suitable variations in composition.

Relative Utility of Methods

The steepest descent method discussed above is relatively efficient in that few evaluations of the objective function are required for each determination of new compositional estimates. However, inasmuch as this method utilizes only first-order information about the objective function, it tends to behave very poorly near the solution so that a large number of iterations produce only negligible progress toward the minimum [Gill et al., 1981, pp. 103-104]. The quasi-Newton method, on the other hand, takes advantage of second-order information about the objective function. Thus it converges relatively rapidly towards a solution, even in the region near the minimum. This method, however, is relatively expensive in terms of computation, with numerous evaluations of the objective function being required for each determination of new compositional estimates. A good strategy for the implementation of these two methods, then, would be to employ the efficient steepest descent method initially and to switch to the rapidly converging quasi-Newton method in the region near the minimum.

APPENDIX C: SOLUTION OF NONLINEAR EQUATIONS

In this section we discuss the application of Newton's method [*cf.* Gerald and Wheatley, 1984, pp. 133-139] to the solution of nonlinear equations. Given a nonlinear function f(x), we wish to find a value of x such that:

$$f(x) = 0 \ . \tag{C-1}$$

If we have some estimate x' of the solution, we may expand the function f about x' in a first-order Taylor series [*cf.* Hurley, 1980, pp. 710-714]:

$$f(x) \approx f(x') + g\left[x - x'\right] \ , \tag{C-2}$$

where g is the first derivative of f evaluated at $x=x'$:

$$g \equiv \left.\frac{df}{dx}\right|_{x=x'} .$$

Thus, from equations (C-1) and (C-2), we have that:

$$f(x') + g\left[x - x'\right] \approx 0 \ ,$$

so that we may obtain our next estimate $\hat{x}$ of the solution from:

$$\hat{x} = x' - \frac{f(x')}{g} \ .$$

We may repeat this process iteratively and refine our compositional estimate to within some arbitrary precision.

Figure Captions

Fig. 1. Isothermal pressure-composition diagram showing computed data boundaries of pyroxene-garnet miscibility gap. Recalibrated data points of Akaogi and Akimoto [1977] denote the high pressure stability limits of the low pressure assemblages (upward-pointing triangles) and the low pressure stability limits of the high pressure assemblages (downward-pointing triangles).

Fig. 2. Isothermal pressure-composition diagram showing computed data boundaries of pyroxene-garnet miscibility gaps. Recalibrated data points of Akaogi and Akimoto [1977] and Akaogi [1978] denote the high pressure stability limits of the low pressure assemblages (upward-pointing triangles) and the low pressure stability limits of the high pressure assemblages (downward-pointing triangles).

Fig. 3. Calculated bulk sound velocity ($\sqrt{\Phi}$) as a function of depth for a suite of mantle bulk compositions along 1700 K (dashed) and 2000 K (solid) isotherms. Composite seismic profile GCA+TNA (dotted) is shown for comparison [see text for references].

TABLE 1. Data Set Consistent with Recalibrated Phase Equilibria

	$Mg_2Si_2O_6$	$Fe_2Si_2O_6$	$CaMgSi_2O_6$	$Mg_4Si_4O_{12}$	$Fe_4Si_4O_{12}$	$Ca_3MgSi_4O_{12}$
phase	opx	opx	cpx	gt	gt	gt
S^{o}_{1000K} (cal/K)	93.51	109.94	96.0	189.13	224.26	190.43
$\alpha_0 \times 10^6$ (K^{-1})	22.031	29.3	21.013	12.552	7.858	7.760
$\left(\frac{d\alpha}{dT}\right)_P \times 10^6$ (K^{-2})	0.010	0.013	0.010	0.026	0.029	0.030
$V_{0,298}$ (cm^3)	62.66	65.94	66.10	114.20	117.06	126.24
K_{0S} (GPa)	103.3	104.2	120.5	163.	168.	164.
$\left(\frac{dK_{0S}}{dP}\right)_T$ raw	4.5-9.5	4.5-9.5	4.5-9.5	3.5-5.5	3.5-5.5	unknown
$\left(\frac{dK_{0S}}{dP}\right)_T$ adj.	5.0	5.0	5.0	4.5	4.5	4.5
γ	1.1	1.1	1.1	1.1	1.1	1.1
δ_S	6.0	6.0	6.0	6.1	5.4	6.0
H^{o}_{1000K} (cal)	-16840.	-6930.	-35320.	816.	27041.	-48038.

Phases are orthopyroxene (opx), clinopyroxene (cpx), and majorite (gt). S^{o}_{1000K} is entropy at 1000 K; α_0, thermal expansion extrapolated to 0 K; $V_{0,298}$, zero-pressure volume at 298 K; K_{0S}, zero-pressure adiabatic bulk modulus at 300 K; γ, Grüneisen ratio; δ_S, Anderson-Grüneisen parameter; H^{o}_{1000K}, enthalpy of formation from oxides at 1000 K and 1 bar. Observed ranges (raw) and best-fit values (adj.) are given for bulk moduli pressure derivatives. [See text for references.]

TABLE 2. Low Pressure Mineralogy (Vol%) of Model Compositions

Phase	Olivine	Peridotite	Pyrolite III	‘‘Piclogite’’	Eclogite
Olv	100	74	54	30	—
Opx	—	14	25	13	—
Cpx	—	3	9	35	57
Gt	—	9	12	22	43

Phases are olivine (olv), orthopyroxene (opx), clinopyroxene (cpx), and garnet (gt). [See text for references.]

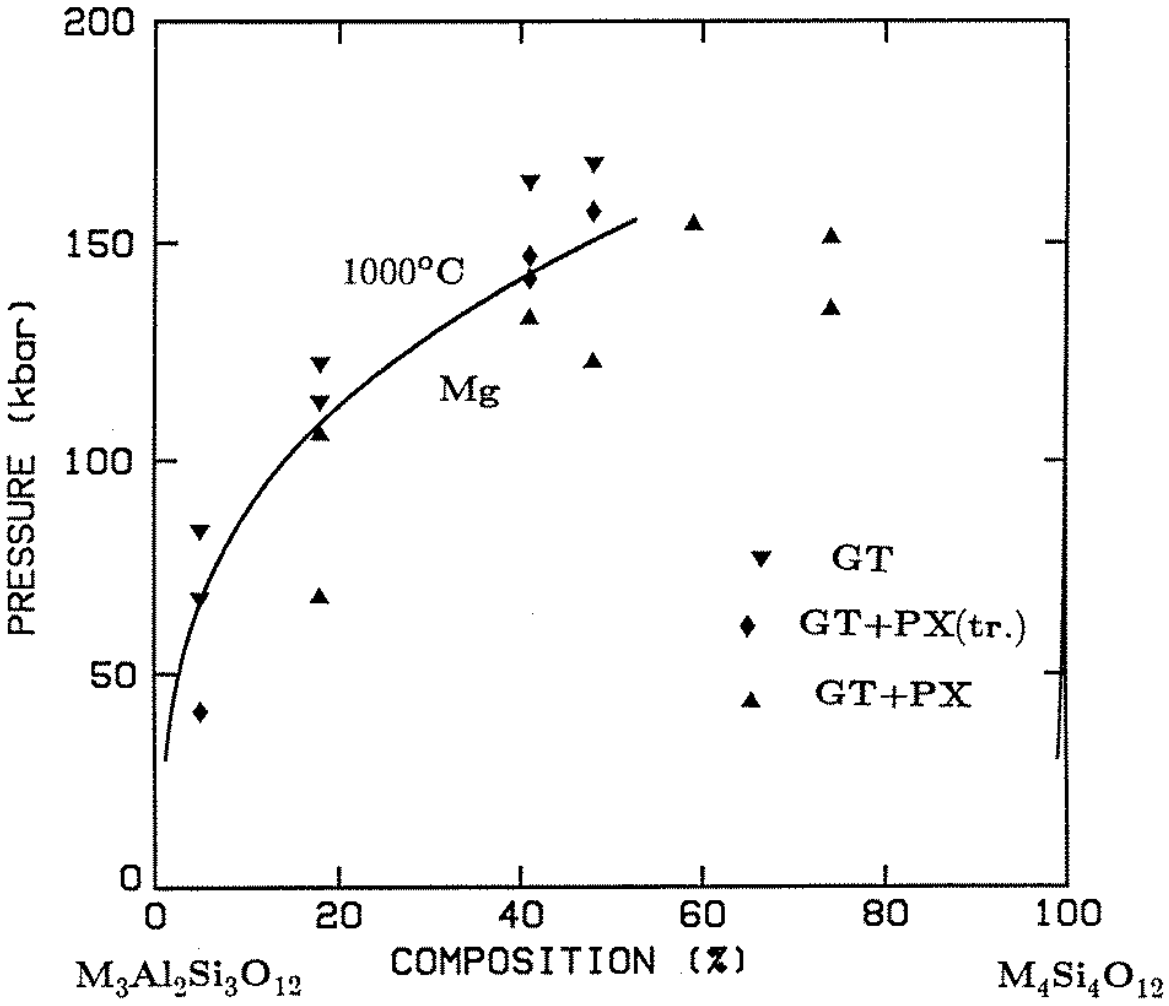
200
150
100
50
0
PRESSURE (kbar)
1000°C
Mg
GT
GT+PX(tr.)
GT+PX
0
20
40
60
80
100
COMPOSITION (%)
$M_3Al_2Si_3O_{12}$
$M_4Si_4O_{12}$

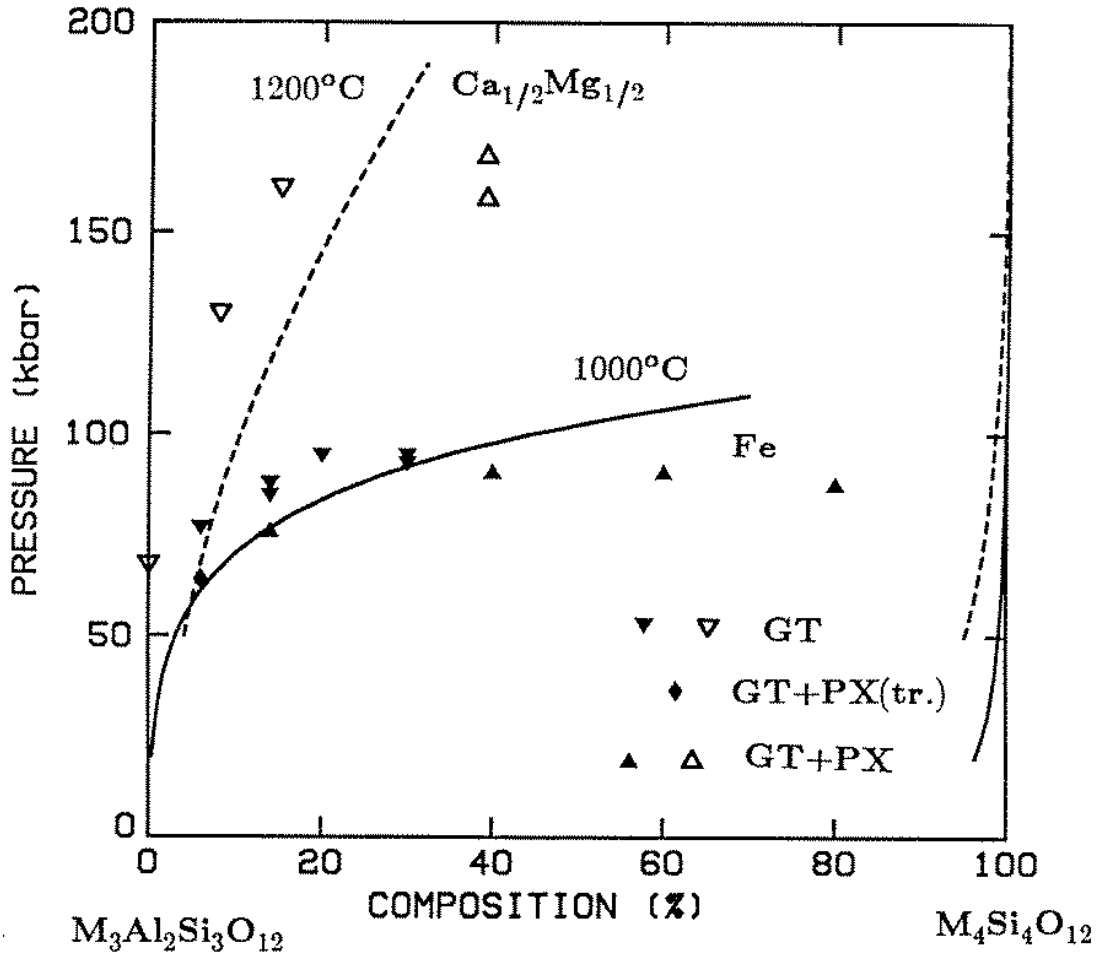
200
150
100
50
0
PRESSURE (kbar)
1200°C
$Ca_{1/2}Mg_{1/2}$
1000°C
Fe
GT
GT+PX(tr.)
GT+PX
0
20
40
60
80
100
COMPOSITION (%)
$M_3Al_2Si_3O_{12}$
$M_4Si_4O_{12}$

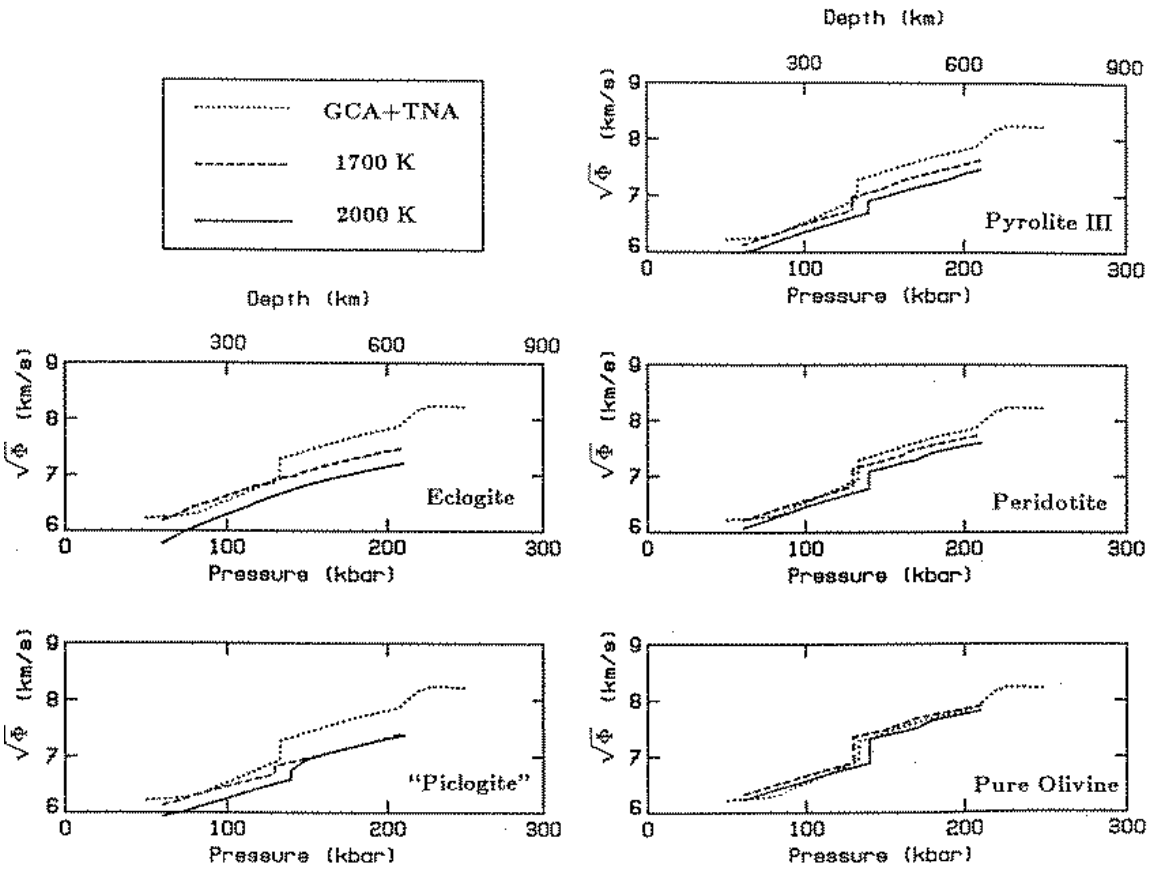
GCA+TNA
1700 K
2000 K
Depth (km)
300
600
900
$\sqrt{\Phi}$ (km/s)
9
8
7
6
0
100
200
300
Pressure (kbar)
Pyrolite III
Eclogite
Peridotite
"Piclogite"
Pure Olivine